

EPR Spectroscopic Study of $S = 1, 2,$ and 3 Spin States of Tris(μ -hydroxo)-Bridged Chromium(III) Dimers

S. KREMER†

Received January 20, 1984

Single-crystal EPR spectra of tris(μ -hydroxo)-bridged dimers $[\text{LCr}(\text{OH})_3\text{L}]_2\text{X}_3 \cdot n\text{H}_2\text{O}$ ($\text{X} = \text{I}^-$, $n = 3$; $\text{X} = \text{ClO}_4^-$, $n = 1$) with point symmetry C_{3h} were recorded at X- and Q-band conditions for different temperatures and field directions. The zero-field splittings of each excited spin state ($S = 1, 2, 3$) in the exchange-coupled system ($-2J = 128 \text{ cm}^{-1}$) could be derived with $|D_1| = 2.28 \text{ cm}^{-1}$, $|D_2| = 0.08 \text{ cm}^{-1}$, and $|D_3| = 0.23 \text{ cm}^{-1}$. Only a small exchange striction must be assumed. In addition, ligand field calculations in trigonal symmetry were used to compare the local zero-field splittings with the d-electronic spectra.

Introduction

Structural and magnetic properties of a large number of bis(μ -hydroxo)-bridged dimeric chromium(III) complexes have been investigated in recent years. Large variations of the singlet-triplet splittings between 0 and 54 cm^{-1} are reported with the Cr-Cr distances ranging from 2.94 to 3.06 \AA . The symmetries of most of these compounds are nearly C_{2v} . The magnetic susceptibility measurements lead to exchange-coupling parameters of the isotropic superexchange between the $S = 3/2$ spin ground states of the two Cr(III) centers averaging the properties of the four different, often well-separated, spin states from $S = 0$ to 3 in the coupled system. For several compounds of the bis(μ -hydroxo)-bridged type,¹ EPR spectroscopy indicates the presence of different spin states with $S \neq 0$. The line width of the numerous signals and the symmetry of the dimers do not allow an unambiguous assignment of the resonances to internal transitions within the $S = 1, 2,$ or 3 spin states. Recently highly symmetric tris(μ -hydroxo) dimers $[\text{LCr}(\text{OH})_3\text{CrL}]_2\text{X}_3 \cdot 3\text{H}_2\text{O}$ ($\text{X} = \text{I}^-, \text{ClO}_4^-$) were structurally characterized² and the magnetic susceptibility data fitted to the antiferromagnetic exchange-coupled dimer model.³ The ligand L is the cyclic amine 1,4,7-trimethyl-1,4,7-triazacyclononane. The crystallographic point symmetry of the whole molecule is C_{3h} with a C_3 axis in the Cr-Cr direction. The dimers are well separated from each other in the lattice. The shortest distance (2.64 \AA) between the Cr ions reported in the dimers results in a triplet-singlet separation of about 140 cm^{-1} for the ClO_4^- salt. At this stage of the investigations only preliminary results of EPR powder spectra have been presented for this compound. In the following sections, particular emphasis is placed on the single-crystal EPR investigations of two compounds with $\text{X} = \text{I}^-$ and ClO_4^- to elucidate the properties of the $S = 1, 2,$ and 3 spin states in terms of the spin-Hamiltonian formalism. In addition, the electronic spectra between 10×10^3 and $30 \times 10^3 \text{ cm}^{-1}$ are considered.

Experimental Section

Sample Preparation. The samples used were kindly supplied by K. Wiegardt. Single crystals of $[\text{Cr}_2(\text{OH})_3\text{L}_2]\text{I}_3 \cdot 3\text{H}_2\text{O}$ and $[\text{Cr}_2(\text{OH})_3\text{L}_2](\text{ClO}_4)_3 \cdot \text{H}_2\text{O}$ were grown in water, resulting in red needles and six-edged plates, respectively.

EPR Measurements. EPR spectra of three single crystals for each compound were obtained at 9 GHz (X-band) and at 35 GHz (Q-band) with a Varian E15 spectrometer using DPPH as internal standard. Spectra were recorded between 3.8 and 300 K at X-band by using a helium-flow cryostat (Oxford Instruments) and between 80 and 300 K in Q-band.

Optical Spectra. Optical spectra in the visible and near-UV region were recorded at 300 K with a DMR 21 spectrometer (C. Zeiss, Oberkochen) in solution (water) and for the solid compounds.

Results and Discussion

The EPR resonance signals of the dimers can be attributed to the transitions in the axially distorted spin $S = 1, 2,$ and 3 excited states of the exchange-coupled system. The EPR spectra for $[\text{LCr}(\text{OH})_3\text{CrL}]\text{I}_3 \cdot 3\text{H}_2\text{O}$ and the measured resonance fields for

Table I. Experimental and Calculated Resonance Field Strengths H_r (in kG) for $[\text{Cr}_2(\text{OH})_3\text{L}_2](\text{ClO}_4)_3 \cdot \text{H}_2\text{O}$ at 300 K in Q- and X-Band for the $S = 1$ State ($|D_1| = 2.25 \text{ cm}^{-1}$, $\bar{g} = 1.98$)

θ	$H_r(35.1 \text{ GHz})$	$H_r(\text{calcd})^a$	$H_r(9.27 \text{ GHz})$	$H_r(\text{calcd})^a$
0	≈ 11.7	11.71 (0.5)	21.00	21.00 (0.5)
30	7.51	7.37 (0.0)		1.93 (0.0)
45	9.29	9.15 (0.1)		2.36 (0.0)
60	≈ 12.80	12.84 (0.4)		3.34 (0.1)
90	21.54	21.60 (1.0)	9.75	9.60 (1.0)

^a In parentheses are given the relative intensities calculated according to common procedures⁷ for 300 K, normalized to unity for $\theta = 90^\circ$ and $S = 1$.

$[\text{LCr}(\text{OH})_3\text{CrL}](\text{ClO}_4)_3 \cdot \text{H}_2\text{O}$ at 300 K are given in Figure 1 and Tables I-III, respectively. For the two compounds investigated, the relative intensities of the experimental resonances are comparable in magnitude.

θ is the angle between the magnetic field vector and the threefold axis C_3 in the Cr-Cr' direction. All spectra are axial with no angular dependence of resonances H_r in the plane perpendicular to C_3 ($\theta = 90^\circ$) and hence reflect the high symmetry, C_{3h} , of the compounds. The line width ΔH_{pp} of the signals at 300 K varies between 250 and 500 G depending on spin S and the field direction. The powder spectra recorded³ correspond to those of the perpendicular plane because these dominate in intensity with respect to those of the parallel orientation. As we use DPPH as an internal standard for the magnetic field calibration and do not verify the linearity of the field scale in the whole range of the applied magnetic field, the experimental error for the resonance field strengths must be assumed as $\pm 100 \text{ G}$ depending on the distance from H_r (DPPH).

Exchange coupling in dimeric chromium(III) complexes with 4A_2 ground states on each center can be described by the isotropic part of the spin Hamiltonian

$$\mathcal{H}_{ex} = -2JS_1S_2 - j(S_1S_2)^2 \quad (1)$$

with the usual meaning of the parameters.³ From susceptibility data³ we derived that the excited spin states are positioned at about $E_1 \approx 140 \text{ cm}^{-1}$ ($S = 1$), $E_2 \approx 408 \text{ cm}^{-1}$ ($S = 2$), and $E_3 \approx 784 \text{ cm}^{-1}$ ($S = 3$). The relative energies can also be roughly calculated from the EPR spectra by comparing the intensities of single resonance lines of the different spin states varying with temperature according to a Boltzmann distribution. For the EPR spectra of pairs of similar ions in addition to the dominant isotropic part of eq 1, the axial symmetry of the system can be introduced by the pair spin Hamiltonian (anisotropic part only)

$$\mathcal{H}_{aniso} = H_1 + H_2 + D_e(3S_{z1} \cdot S_{z2} - \frac{1}{4}) \quad (2)$$

with

$$H_1 = \beta\mathbf{H} \cdot \mathbf{g} \cdot \mathbf{S}_1 + D(S_{z1}^2 - \frac{3}{4}) \quad (3)$$

- (1) Glerup, J.; Hodgson, D. J.; Pedersen, D. *Acta Chem. Scand., Ser. A* **1983**, *A37*, 161.
 (2) Wiegardt, K.; Chaudhuri, P.; Nuber, B.; Weis, J. *Inorg. Chem.* **1982**, *21*, 3086.
 (3) Bolster, D. E.; Gülich, P.; Hatfield, W. E.; Kremer, S.; Müller, E. W.; Wiegardt, K. *Inorg. Chem.* **1983**, *22*, 1725.

† Present address: NBC Defense Research Institute, D-3042 Munster, FRG.

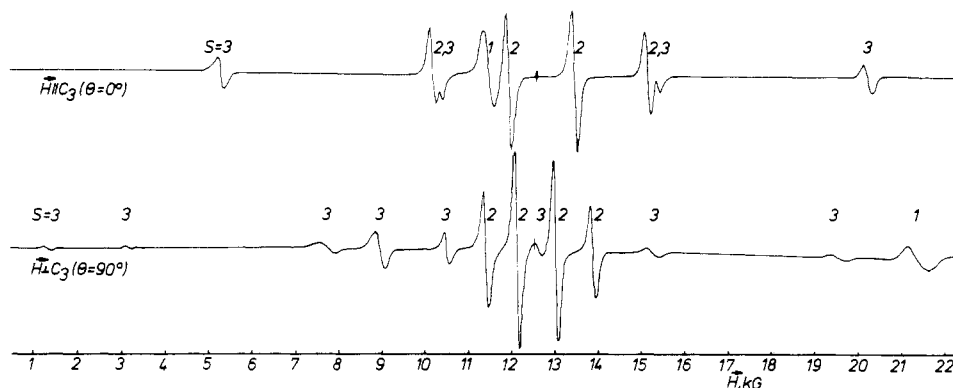


Figure 1. EPR spectra of $[\text{C}_2(\text{OH})_3\text{L}_2]_{1,3,3}\text{H}_2\text{O}$ at 300 K for Q-band ($\nu = 35.1$ GHz) and field directions H (in kG) of $\theta = 0$ and 90° corresponding to $H \parallel C_3$ and $H \perp C_3$, respectively (DPPH at $H = 12.51$ kG).

Table II. Experimental and Calculated Resonance Field Strengths H_r (in kG) for $[\text{Cr}_2(\text{OH})_3\text{L}_2](\text{ClO}_4)_3 \cdot \text{H}_2\text{O}$ at 300 K in Q- and X-Band for the $S = 2$ State ($|D_2| = 0.05 \text{ cm}^{-1}$, $\bar{g} = 1.98$)

θ	$H_r(35.1 \text{ GHz})$	$H_r(\text{calcd})^a$	$H_r(9.27 \text{ GHz})$	$H_r(\text{calcd})^a$
0	11.06, 12.08, 13.05, 14.13	11.01 (0.29), 12.09 (0.43), 13.17 (0.43), 14.25 (0.29)	1.71, 2.91, 3.85, 4.91	1.71 (0.29), 2.80 (0.43), 3.88 (0.42), 4.96 (0.29)
30	11.61, 12.33, 12.99, 13.49	11.55 (0.29), 12.32 (0.44), 13.00 (0.45), 13.57 (0.30)	2.06, 3.12, 3.79, 4.06	2.04 (0.27), 3.11 (0.41), 3.79 (0.43), 4.08 (0.32)
45	12.23, 12.50, 12.85	12.14 (0.32), 12.53 (0.49), 12.80 (0.51), 12.94 (0.35)	2.61, 3.41, 3.54	2.53 (0.27), 3.38 (0.84), 3.56 (0.51)
60	≈ 12.4 – 12.6	12.36 (0.42), 12.57 (0.62), 12.72 (0.60), 12.76 (0.39)	2.97, ≈ 3.3	2.92 (0.46), 3.26 (0.95), 3.51 (0.56)
90	11.88, 12.40, 12.88, 13.38	11.84 (0.52), 12.34 (0.79), 12.87 (0.79), 13.45 (0.52)	2.65, 2.97, 3.52, 4.10	2.58 (0.52), 2.98 (0.78), 3.49 (0.78), 4.16 (0.55)

^a See footnote *a* in Table I.

Table III. Experimental and Calculated Resonance Field Strengths H_r (in kG) for $[\text{Cr}_2(\text{OH})_3\text{L}_2](\text{ClO}_4)_3 \cdot \text{H}_2\text{O}$ at 300 K in Q- and X-Band for the $S = 3$ State ($|D_3| = 0.24 \text{ cm}^{-1}$, $\bar{g} = 1.98$)

θ	$H_r(35.1 \text{ GHz})$	$H_r(\text{calcd})^a$	$H_r(9.27 \text{ GHz})$	$H_r(\text{calcd})^a$
0	0.48, 4.75, 10.20, 15.45, 20.45	0.36 (0.1), 4.84 (0.1), 10.03 (0.15), 15.22 (0.15), 20.42 (0.1)	0.66, 4.6, 5.89, 11.1, 16.43	0.74 (0.15), 4.46 (0.1), 5.93 (0.15), 9.65 (0.1), 11.12 (0.1), 16.32 (0.1)
30	0.63, 3.86, 4.02, 6.08, 6.78, 7.15, 9.18, 13.0, 14.7, 16.10, 16.54	0.41 (0.1), 3.82 (0.01), 4.07 (0.01), 4.66 (0.01), 5.98 (0.05), 6.27 (0.05), 6.67 (0.1), 9.12 (0.05), 12.84 (0.1), 15.09 (0.1), 16.08 (0.13), 16.62 (0.1)	0.49, 2.04, 4.3, 7.16	0.57 (0.1), 2.04 (0.27), 4.38 (0.07), 7.11 (0.03)
45	0.69, 2.24, 2.91, 4.38, 5.58, 7.10, 8.39, 10.0, 10.64, 14.35	0.49 (0.07), 2.28 (0.01), 2.68 (0.01), 3.02 (0.01), 4.4 (0.03), 5.65 (0.01), 7.08 (0.05), 8.41 (0.01), 10.09 (0.1), 10.71 (0.12), 12.55 (0.2), 14.35 (0.3)	0.44, 1.21, 2.01, 4.24, 7.0	0.5 (0.07), 1.24 (0.18), 1.92 (0.03), 2.00 (0.13), 4.20 (0.11), 6.52 (0.07), 6.86 (0.08)
60	1.0, 2.56, 5.06, 6.43, 8.30, 8.65, 10.15, 12.0, 14.19	0.65 (0.06), 2.50 (0.02), 5.01 (0.01), 8.21 (0.04), 8.71 (0.13), 10.23 (0.2), 12.12 (0.2), 13.99 (0.12), 14.25 (0.2)	0.41, 0.87, 1.91, 6.7	0.46 (0.04), 0.9 (0.19), 1.91 (0.14), 6.71 (0.06)
90	1.06, 2.96, 7.43, 8.75, 10.40, 12.5, 15.27, 19.77	1.18 (0.01), 1.69 (0.06), 3.01 (0.02), 7.52 (0.14), 8.82 (0.21), 10.44 (0.24), 12.58 (0.24), 15.28 (0.21), 19.69 (0.14)	0.66, 1.81, 4.69, 10.6	0.71 (0.2), 1.81 (0.15), 4.64 (0.15), 10.42 (0.2)

^a See footnote *a* in Table I.

for the single ion 1 and similar Hamiltonian for ion 2.⁴ It is this part of the whole Hamiltonian that determines the positions of EPR resonance lines. The first term on the right-hand side of eq 3 represents the energy in the applied external magnetic field. D stands for the usual second-order crystal field terms of axial symmetry in the spin-Hamiltonian formalism, which can be transformed to local crystal field parameters of trigonally distorted, six-coordinated Cr(III) complexes via ligand field calculations. The method to calculate ligand field energies of the d^3 configuration in trigonal symmetry with spin-orbit coupling is described elsewhere.⁵ The parameter D_e of eq 2 in the pure spin-coupled model represents the anisotropic part of the exchange interaction and reflects the directional properties of orbitals coupled to the spins by spin-orbit coupling. This term includes several contri-

butions such as true dipolar interaction, pseudodipolar exchange, and others.⁴ The different parts are separable only on the theoretical basis discussed, for example, by Kanamori.⁶ As in our case the term in J is much greater than D , D_e , or βH , the system is most conveniently described in terms of the total spins $S = S_1 + S_2$ ($S = 0, 1, 2, 3$); each spin state ($S \neq 0$) undergoes a zero-field splitting of axial symmetry. The relevant part of the total spin Hamiltonian can now be described by

$$\mathcal{H} = D_S(Z^2 - \frac{1}{3}S(S+1)) + E_S \quad (4)$$

with $S = 0, 1, 2$, or 3 and the energy D_S of the well-separated spin states given above in eq 1. The parameters D_S for each spin state are related to the parameters D_e and D of eq 2 and 3 by

$$\begin{aligned} D_1 &= 5.1D_e - 2.4D & D_2 &= 1.5D_e \\ D_3 &= 0.6D_e + 0.4D \end{aligned} \quad (5)$$

(4) Owen, J.; Harris, E. A. In "Electronic Paramagnetic Resonance"; Geschwind, S., Ed.; Plenum Press: New York, 1972.

(5) König, E.; Kremer, S. "Ligand Field Diagrams"; Plenum Press: New York, 1976.

(6) Kanamori, J. In "Magnetism"; Rado, G. T., Suhl, H., Eds.; Academic Press: New York, 1963; Vol. 1.

However, since the geometry of the dimer need not be the same for each spin state (exchange striction), especially if the exchange interaction is large, eq 5 does not necessarily hold. Assuming an isotropic g factor of $\bar{g} = 1.98$, we calculated the resonance field strength in the range of $H = 0$ –22 kG for X- and Q-band ($h\nu = 0.31$ and 1.17 cm^{-1} , respectively) on the basis of eq 4 by direct diagonalization of the energy matrices in steps of 50 G according to common procedures. The relative transition probabilities were calculated by means of magnetic dipole operators perpendicular to the applied magnetic field H , i.e. in the plane of the oscillating field.⁷ The calculated transition probabilities serve to estimate the possibility of experimental observation. Additionally, the experimental relative intensities are used to derive the energy differences between the spin states of the exchange-coupled system from the corresponding Boltzmann factors. As there exist considerable line width variations in the signals with temperature, this procedure can lead only to approximate values of the energy difference compared to the data extracted from the magnetic measurements.

S = 1 State. For the ClO_4^- and Γ^- compounds at 300 K the resonance field strengths are calculated with $|D_1| = 2.25$ (± 0.02) cm^{-1} and $|D_1| = 2.22$ (± 0.02) cm^{-1} , respectively. At $\theta = 0^\circ$ in Q-band, the $S = 1$ transitions are obscured by $S = 2$ transitions but clearly follow the calculated θ variation up to $\theta = 90^\circ$ in the limit of experimental error (Table I).

In addition, the experimental spectra for the ClO_4^- compound are in agreement with the expected increase of $H_r > 21.0$ kG in X-band for small deviations of θ from $\theta = 0^\circ$; e.g. for $\theta = 4^\circ$, $H_r = 21.72$ kG (calculated $H_r = 21.88$ kG). As the experimental line width increases enormously for $\theta > 5^\circ$, we could not follow this signal to the highest possible field strength of $H \approx 25$ kG. The transition probability calculated for $\theta = 30, 45$, or 60° in X-band is about 1% of that in the $\theta = 0$ or 90° directions. Because the quantum $h\nu$ is smaller than the zero-field splitting D_1 of the $S = 1$ state, the resonance field for the Q-band is lower than that at X-band for $H \parallel C_3$. This can be further proven by a measurement at 62 GHz (V-band, $h\nu = 2.07$ cm^{-1} , 300 K) where this signal is found at $H_r = 2.24$ kG.

At lower temperatures of about 80 K slight increases of $|D_1| = 2.30$ cm^{-1} and $|D_1| = 2.25$ cm^{-1} for the ClO_4^- and Γ^- compounds, respectively, are derived. At $T < 30$ K the signals vanish completely.

S = 2 State. The variation of the resonance field strengths for the ClO_4^- compound is shown in Table II for the Q- and X-band together with the resonance positions calculated with $|D_2| = 0.05$ (± 0.01) cm^{-1} (300 K). For the Γ^- compound, two representative spectra [$\theta = 0$ and 90° (300 K) in Q-band] are depicted in Figure 1. From the angular dependence of the resonance fields, an axial parameter of $|D_2| = 0.08$ (± 0.01) cm^{-1} is calculated. In both compounds the superposition of different lines from $S = 2$ and $S = 3$ slightly obscures the single $S = 2$ resonances in the Q-band for some θ values, but the combined recalculation of experimental resonance fields at two frequencies and different magnetic field directions overcomes this difficulty. The four lines seen for $\theta = 0^\circ$ and 90° in X- and Q-band have an intensity ratio of the outer pair to the inner pair of 2:3, which agrees very well with the calculated values if Lorentzian line shapes are assumed. If the temperature is lowered to about 80 K, the parameters become $|D_2| = 0.05$ and 0.09 cm^{-1} for ClO_4^- and Γ^- compounds, respectively. We can use the intensity ratios of two suitable, well-resolved lines from the $S = 1$ and $S = 2$ manifold at 300 and 80 K as a rough estimate of the $S = 1$ and $S = 2$ energy separation. No internal intensity standard is thus required to derive the energy interval between both states. As we assume, for simplicity, Lorentzian line shapes, only approximate values for the intensities are obtained. With $I_1(300 \text{ K}) \approx 0.144$, $I_1(80 \text{ K}) \approx 4.53$, $I_2(300 \text{ K}) \approx 0.056$, and $I_2(80 \text{ K}) \approx 0.075$ (in arbitrary units, Q-band, $\theta = 90^\circ$) an energy separation of $E_2 - E_1 \approx 230$ cm^{-1} results for the ClO_4^- compound, in reasonable agreement with the value of

268 cm^{-1} derived from susceptibility data. In the same way a separation energy of $E_2 - E_1 \approx 170$ cm^{-1} was deduced from $I_1(300 \text{ K}) \approx 0.061$, $I_1(80 \text{ K}) \approx 0.035$, $I_2(300 \text{ K}) \approx 0.175$, and $I_2(80 \text{ K}) \approx 0.100$ (Q-band, $\theta = 45^\circ$) for the Γ^- compound. This corresponds to a slightly smaller exchange-coupling constant of $J \approx -43$ cm^{-1} , which has not yet been determined from magnetic data.

S = 3 State. Numerous resonances are detected for the $S = 3$ state, which are tabulated for different θ values at X- and Q-band conditions (300 K) for the ClO_4^- compound in Table III. The calculated relative intensities are listed; they agree in order of magnitude with those experimentally found. The axial parameter $|D_3| = 0.24$ (± 0.005) cm^{-1} fits the measured spectra if one takes into account the extreme sensitivity of signal positions to the variation of field direction as well as some misalignment of the crystals. No change of D_3 with lowering of temperature is observed. For $X = \Gamma^-$, Figure 1 shows the resonances for an applied field strength from $H = 1$ to 22 kG (Q-band, 300 K), which corresponds to $|D_3| = 0.230$ (± 0.005) cm^{-1} . Between $T = 150$ and 100 K the $S = 3$ resonances are strongly reduced in intensity, until at 80 K no signal from the $S = 3$ state can be observed anymore. Raising the temperature to 400 K increases the $S = 3$ population with a small increase of $|D_3| = 0.25$ cm^{-1} only for the Γ^- compound.

The axial parameters derived from the EPR spectra characterize the zero-field splittings of the well-separated spin states of the coupled system. D_e and D are only equal for the different spin states (eq 5) if one introduces the further assumption of equal distances in the molecule for each occupied spin state. The parameters approximately obey eq 5 only if one takes account of the undetermined signs according to $D_1 \lesssim 0$ and $D_3 \gtrsim 0$, which lead for the Γ^- compound to the calculated value of $|D_e| = 0.08$ (± 0.005) cm^{-1} , comparable in magnitude to the experimental value $|D_e| = 0.05$ (± 0.01) cm^{-1} from $|D_2| = 0.08$ cm^{-1} above. Thus exchange striction seems to be very small and is neglected in the following considerations. If one assumes D_e to include true dipolar interaction $D_d = -\beta^2 \bar{g}^2 / r_{12}^3$ and pseudodipolar exchange D_E ,⁴ we may derive a value of the latter parameter for the Γ^- compound on the basis of a calculated dipolar interaction parameter $D_d = -0.09$ cm^{-1} ($r(\text{Cr}-\text{Cr}) = 2.64$ \AA). Two parameter values of D_E (0.14 or 0.04 cm^{-1}) are calculated depending on the sign of D_e . Following Kanamori,⁶ the magnitude of this effect should be of order $2|J|(\zeta/\Delta)^2 \approx 0.01$ cm^{-1} , with the spin-orbit coupling parameter $\zeta = 200$ cm^{-1} and the octahedral splitting parameter $\Delta = 20000$ cm^{-1} of the single Cr(III) entities derived from electronic spectra (see below). Obviously these contributions are of the magnitude of the experimental error and hence cannot be considered.

Without exchange striction, for the Γ^- compound, the zero-field splitting $|D| = 0.755$ cm^{-1} for the 4A_2 ground state of the single Cr(III) centers is calculated from $D_1 = 2.22$ cm^{-1} and $D_3 = -0.23$ cm^{-1} . The magnitude of the local axial distortion is thus comparable with that of the trigonally distorted $\text{Cr}(\text{acac})_3$ ($|D| = 0.59$ cm^{-1}).⁷ The D parameter will now be discussed in terms of the crystal field parameters of the mononuclear trigonally distorted six-coordinated Cr(III) complex.

Electronic Spectra. The absorption spectrum for the ClO_4^- compound in solution has already been reported.² Additionally, we have now observed several sharp bands of lower intensity at $(15\text{--}16) \times 10^3$ cm^{-1} in the solution as well as in the solid.

Reflection spectra for $X = \Gamma^-$ at 300 K are depicted in Figure 2. They agree completely with the solution spectra and with the spectra of the ClO_4^- compound.

Usually spin-allowed and spin-forbidden d-d bands are observed essentially at the same positions in dimers as in the mononuclear complex though the intensity gain of the spin-forbidden transitions may be considerable.⁸ We may thus correlate the observed electronic spectra directly with the d-d transitions in the ligand field model of configuration d^3 with trigonal distortion C_{3v} , in accord with the structural results.² Accordingly, the broad band at $\approx 20 \times 10^3$ cm^{-1} is assigned to the first spin-allowed transition $^4A_2(t_2^3) \rightarrow ^4T_2(t_2^2e)$ and leads to the octahedral splitting

(7) Al'tshuler, S. A.; Kozyrev, B. M. "Electron Paramagnetic Resonance in Compounds of Transition Elements"; Wiley: New York, 1974.

(8) Decurtins, S.; Güdel, H. U. *Inorg. Chem.* **1982**, *21*, 3598.

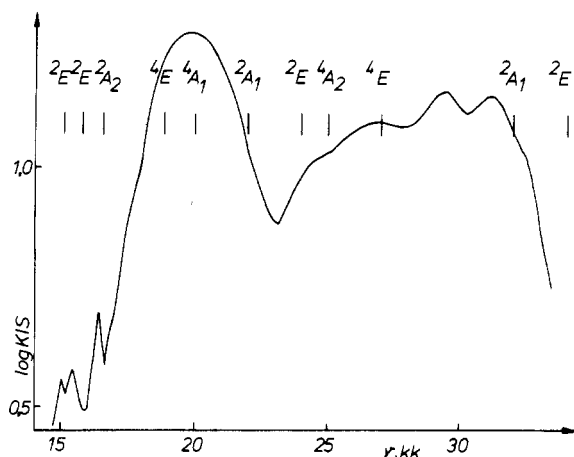


Figure 2. Optical spectrum of $[\text{Cr}_2(\text{OH})_3\text{L}_2]\text{I}_3 \cdot 3\text{H}_2\text{O}$ at 300 K in the visible and near-UV region in reflection together with the term assignments calculated for the configuration d^3 with a trigonal ligand field.

parameter $\Delta_{\text{oct}} \approx 20\,000 \text{ cm}^{-1}$, which lies between those of the pure $\text{Cr}^{\text{III}}\text{-O}_6$ and $\text{Cr}^{\text{III}}\text{-N}_6$ chromophores.⁹ The sharp band at 15.0×10^3 , 15.4×10^3 and $16.3 \times 10^3 \text{ cm}^{-1}$ should then correspond to the first spin-forbidden transitions to the ${}^2\text{E}$, ${}^2\text{T}_2(t_2^3)$ terms. The broad bands at 25×10^3 and $27 \times 10^3 \text{ cm}^{-1}$ have to be correlated with the second spin-allowed transition to the trigonal-split terms of ${}^4\text{T}_2(t_2^2e)$. The higher absorptions at $\approx 30 \times 10^3 \text{ cm}^{-1}$ originate possibly from spin-forbidden transitions with high-intensity gain from exchange coupling. For the octahedral case, by calculation in the strong-field coupling scheme with complete d^3 configuration, the Racah parameters $B = 700$ and $C = 3400 \text{ cm}^{-1}$ can be approximated. The trigonal distortion that is indicated in the optical spectra can be specified by use of the EPR spectroscopically determined zero-field splitting of the ${}^4\text{A}_2$ ground state $\Delta E = 2D \approx 1.51 \text{ cm}^{-1}$. This splitting of the ground level is introduced via second-order spin-orbit coupling and trigonal splitting of the excited states.

(9) Jørgensen, C. K. "Oxidation Numbers and Oxidation States"; Springer Verlag: Berlin, 1969.

From structural information, the C_{3v} symmetry of the CrO_3N_3 entity is known, with the angle $\theta = 48$ and 50° between the C_3 axes and the Cr-O and Cr-N directions, respectively. If we use the concept of the AO model with an averaged σ -bonding parameter e_σ for Cr-O and Cr-N and only a small π -bonding contribution ($e_\pi = 0.1e_\sigma$), we derive a reasonable value of $e_\sigma = 7800 \text{ cm}^{-1}$ ($\theta = 54^\circ 44'$).¹⁰ With the crystallographic angle of $\theta = 48^\circ$, the AOM parameters and the spin-orbit coupling constant of $\zeta = 200 \text{ cm}^{-1}$ from a specific calculation in the d^3 trigonal strong-field coupling scheme,⁵ the zero-field splitting $\Delta E = 1.54 \text{ cm}^{-1}$ of the ${}^4\text{A}_2$ ground state results in reasonable agreement with the EPR spectroscopic results. The AOM parameters are transformed to the final traditional parameters $Dq = 1770$, $Dt = 300$, and $Ds = -1260 \text{ cm}^{-1}$ of ref 5. The calculated term sequences are added in Figure 2. The corresponding one-electron configurations of the given trigonal states can easily be correlated to the common octahedral t_2 and e one-electron orbitals. The trigonal distortion characterized above by $\theta = 48^\circ$ splits the octahedral ${}^4\text{T}_2(t_2^3)$ and ${}^4\text{T}_1(t_2^2e)$ states into essentially two components separated by 1200 and 1800 cm^{-1} , respectively, which seem only resolved in the powder spectra for the latter. As we use the same B and C parameters for different one-electron configurations, the higher doublet states at $\approx 30 \times 10^3 \text{ cm}^{-1}$ are not so well fitted to the experimental spectra.

In bis(μ -hydroxo)-bridged Cr(III) dimers, the intensity of their spin-forbidden transitions increases with J ,⁸ and one should suppose the same trend in our case of much larger exchange coupling. This corresponds to the observed strong unresolved absorption bands in the near-UV region. They should be characteristic for exchange-coupled systems and are much less in intensity for the more weakly coupled bis(μ -hydroxo)-bridged species but appear in both cases at almost the same position. Possibly single-crystal polarized absorption spectra could clear up this weak point in the interpretation of the electron excitations given above.

Acknowledgment. We thank Dr. A. Ozarowski and Prof. D. Reinen for helpful discussions.

Registry No. $[\text{Cr}_2(\text{OH})_3\text{L}_2]\text{I}_3$, 94517-77-8; $[\text{Cr}_2(\text{OH})_3\text{L}_2]\text{ClO}_4$, 94500-15-9.

(10) Glerup, J.; Mønstedt, O.; Schäffer, C. E. *Inorg. Chem.* **1976**, *15*, 1399.

Contribution from the Department of Chemistry, McMaster University, Hamilton, Ontario, Canada L8S 4M1

A ^{119}Sn Mössbauer Study of Some Nonclassically (Cluster) and Classically Bonded Zintl Anions

THOMAS BIRCHALL,* ROBERT C. BURNS, LESLEY A. DEVEREUX, and GARY J. SCHROBILGEN*

Received December 12, 1983

Tin-119 Mössbauer spectra have been recorded for the following cluster (i.e., nonclassically) bonded Zintl anions, $[\text{Sn}_3]^{2-}$, $[\text{Sn}_9]^{4-}$, $[\text{TiSn}_3]^{5-}$, and $[\text{Sn}_2\text{Bi}_2]^{2-}$, and the data interpreted in terms of the known X-ray crystallographic information. Spectra for the following classically bonded Zintl anions, $[\text{SnSe}_4]^{4-}$, $[\text{SnTe}_4]^{4-}$, and $[\text{SnSe}_{3-x}\text{Te}_x]^{2-}$ ($x = 0-3$, $z = 1, 2$), have also been measured. The $[\text{SnSe}_4]^{4-}$ and $[\text{SnTe}_4]^{4-}$ species are shown to have tin environments slightly distorted from tetrahedral symmetry while $[\text{SnSe}_{3-x}\text{Te}_x]^{2-}$ species are shown to be much more distorted.

Introduction

A number of the heavy main-group elements form intermetallic phases with sodium or potassium that are soluble in liquid ammonia or ethylenediamine (en). About 50 years ago, Zintl and co-workers described electrochemical studies on NH_3 solutions of such sodium alloys and, together with the results of exhaustive alloy extractions, several homopolyatomic anions, namely Sn_9^{4-} , Pb_9^{4-} , Bi_5^{3-} , Sb_7^{3-} , and Te_4^{2-} amongst others, were identified.¹⁻³

These have become known as Zintl anions. Attempts to isolate the salts of these anions by evaporation of the solvent resulted in the formation of amorphous products or reversion to a known binary alloy phase(s) in each case. However, fairly recently Kummer and Diehl⁴ did succeed in isolating crystalline material of composition $\text{Na}_4\text{Sn}_9 \cdot 6-8\text{en}$ from ethylenediamine solutions. This was found to be diamagnetic, and ^{119}Sn Mössbauer measurements showed only one broad resonance with an isomer shift of $+0.15$

(1) Zintl, E.; Goubeau, J.; Dullenkopf, W. *Z. Phys. Chem., Abt. A* **1931**, *154*, 1.

(2) Zintl, E.; Harder, A. *Z. Phys. Chem., Abt. A* **1931**, *154*, 47.

(3) Zintl, E.; Dullenkopf, W. *Z. Phys. Chem., Abt. B* **1932**, *16*, 183.

(4) Kummer, D.; Diehl, L. *Angew. Chem., Int. Ed. Engl.* **1970**, *9*, 895.